Using the values of the energies of beta- and gamma-rays as determined in this paper, the energy level scheme shown in Fig. 9 has been constructed. Energy-wise, there is excellent agreement among all the components of the scheme. The level diagram offered here differs from that of Metzger and Deutsch[13] in putting the 637-kev gamma-ray in cascade with the 80-kev line. Indeed this is required by the new determination of the energy of the low energy group. The branching ratio for the two beta-ray groups is the same as that of Metzger and Deutsch. The relative intensities of the lines were calculated with the help of the Gray curves and yield the following values: $I_{637}=14.2$, $I_{363}=82.5$, and $I_{282}=3.7$ quanta per hundred disintegrations. The ratio $I_{637}/(I_{363}+I_{282})=14.2/86.2$ agrees very well with the ratio of the intensities of the two beta-ray groups. Making use of the proposed disintegration scheme, the relative intensity of the low energy line should be $I_{80}=I_{637}+I_{282}=17.9$ quanta per hundred disintegrations.

The internal conversion coefficients of the lines at 80, 282, and 363 kev have been calculated and are given in Table II together with the ratio N_K/N_L, in those cases in which this quantity could be determined. A search was made for internal conversion electrons connected with the line at 637 kev but none could be found.

This research was assisted by the joint program of the ONR and the AEC. The authors wish to thank Professor L. L. Merritt, of the Department of Chemistry, for valuable help with the chemical separations.

Note added in proof.—Professor K. Siegbahn has informed us in a private communication that he has also investigated the spectrum of Sb^{125}. He has found all of the lines found by us except that at 0.125 Mev and in addition a line at 0.035 Mev. The energies of the lines determined by both investigations agree to better than 5 percent.

In regard to the 165 kev line observed in I^{131}, Brosi, DeWitt, and Zeldes (Phys. Rev. **75**, 1615 (1949)) have shown that a metastable Xe^{131}, of about 12 day half-life, grows from I^{131}. This substance emits an internally converted gamma-ray of energy 165 kev. The exact position of this line in the level scheme must await further investigation.

PHYSICAL REVIEW VOLUME 76, NUMBER 1 JULY 1, 1949

Neutron Cross Sections at 115 ev and 300 ev—I

C. T. HIBDON AND C. O. MUEHLHAUSE
Argonne National Laboratory, Chicago, Illinois

(Received March 18, 1949)

Total neutron cross sections for a number of elements were measured at 115 ev and 300 ev with an energy resolution of approximately 10 percent. The cross sections were separated into two parts: a resonance cross section and an asymptotic cross section. The first cross section represented the effect of a neutron resonance in the material studied overlapping the detector. The second cross section was identified either as the potential scattering cross section, or a minimum cross section in the neighborhood of a resonance.

I. INTRODUCTION

MANY neutron cross sections as a function of neutron energy have been made using instruments having low resolution above 100 ev. It is the purpose of this paper to describe a series of measurements of total neutron cross sections made at two specific energies, but with the high resolution provided by the resonance scattering of Co[1] and Mn.[2] These materials resonantly scatter neutrons at 115 ev and 300 ev respectively, and have therefore been used to detect neutrons at these energies.

II. APPARATUS AND FLUX CONDITIONS

The equipment used was constructed in 1946–47 under the direction of Alexander Langsdorf, Jr.[1,3] It consisted of an annular enriched $BF_3-4\pi$ proportional neutron counter through which a collimated beam of cadmium filtered neutrons from the Argonne heavy water pile could pass. The neutrons were conducted through the center of the chamber in an evacuated tube (see Fig. 1) and gave an appreciable counting rate only when a scattering foil (termed the "detector") was placed in the center of the chamber transverse to the beam. Due to the presence of a paraffin reflector the counter sensitivity fell off logarithmically with neutron energy (from ~13.5 percent at thermal energies to ~1.7 percent at mean fission energies).

The cadmium filtered neutron flux from the pile obeyed the usual dE/E distribution, but because of the particular way in which the chamber sensitivity varied with neutron energy, the flux was regarded as $dE/E^{1.12}$. That is, a flat detector ($d\sigma_s/dE\simeq 0$) such as Be or C provided a counting rate *vs.* neutron energy which followed a $dE/E^{1.12}$ distribution. A graphical analysis of the experimentally determined sensitivity function ($a-b\log E$) showed that the effective number of natural logarithmic cycles in the neutron spectrum from a flat detector was 8.3. This was used to obtain the power function given above.

Assuming a different sensitivity function of the form

[1] S. Harris, A. Langsdorf, and F. Seidl, Phys. Rev. **72**, 866 (1947); Wu, Rainwater, and Havens, Phys. Rev. **71**, 174 (1947).
[2] M. Goldhaber and A. Yalow, Phys. Rev. **69**, 47 (1946); N. Barbre and M. Goldhaber, Phys. Rev. **71**, 141 (1947); Seidl, Harris and Longsdorf, Phys. Rev. **72**, 168 (1947); Rainwater, Havens, Wu, and Dunning, Phys. Rev. **71**, 65 (1947).
[3] A. Langsdorf, Jr., to be published in Rev. Sci. Inst.

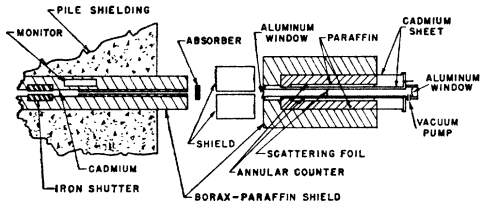

FIG. 1. Schematic diagram of annular counter and shields.

$1/E^{n+1}$ and equating:

$$(0.5)^n \int dE/E^{n+1} = 8.3$$

where the integral is taken from the Cd cut-off energy (0.5 ev) to the mean fission energy (1.5×10^6 ev) yields $n=0.12$.

Pulses from the annular counter and a fission neutron monitor counter (see Fig. 1) were recorded simultaneously. The counting rates were corrected for the chamber-circuit deadtime of $15\mu s$.

III. PREPARATION OF SAMPLES

The samples used were of the greatest purity obtainable, most being of "reagent grade." All substances measured were spectroscopically analyzed for traces of impurities, with special emphasis on Co and Mn. Because of the high self-indication cross section of Co and Mn ($\sim3000b$) it was necessary to use materials having less than 0.03 percent of these contaminants.

The elemental form of the material was chosen whenever possible. Pure metals were either cast into cylindrical shape, pressed into pellets or canned in metal containers having 4 mil thick aluminum ends. Iodine oxides and the fluorides were similarly canned; Hg and Br were measured in cylindrical soft glass containers having thin windows. Corrections of the order of 1 percent were made for the absorption of the containers.

IV. RESOLUTION OF THE DETECTORS

The principal measurements were made by placing thin Co(24.8 mg/cm²) or thin Mn(19.5 mg/cm²) in the center of the annular scattering chamber and determining the counting rate *vs.* thickness of absorbing material studied. Background counting rates (~10 percent of the total rate) were also measured without the detector foil in place. Measurements were first made, however, using Co and Mn as absorbers. That is, the Co-detected Co transmission curve and the Mn-detected Mn transmission curves were first measured to determine the fractions of resonantly and potentially scattered neutrons. The observed intercept ratios of initial to asymptotic parts (Figs. 2 and 3) are approximately the resolving powers of the foils. They are for Co and Mn respectively: 5.2 and 10.6. The resolution of the foils were also determined by measuring their epi-cadmium scattering cross sections, $\sigma_{\text{epi-Cd}}$, (by comparison with carbon in the epi-cadmium beam), and comparing $\sigma_{\text{epi-Cd}}$ with the potential scattering cross section, σ_p:

Co: $\sigma_{\text{epi-Cd}}=35.4b$ $\sigma_p=7.2b$ $\therefore$res/pot$\simeq4$
Mn: $\sigma_{\text{epi-Cd}}=34.2b$ $\sigma_p=3.5b$ $\therefore$res/pot$\simeq9$.

Average values of 4.5 and 9.8 were used for Co and Mn respectively.

Without the presence of potential scattering an infinitely thin foil would have an ideal resolving power, E_0/Γ, or 30 and 20 for Co and Mn respectively. This resolution was approached by subtracting the properly-scaled flat-detected, i.e., C-detected, transmission curve from the Co- and Mn-detected transmission curves. Actually a somewhat simpler procedure than this was followed (see Section V) with a resulting energy detection band width $<E_0/10$ for both foils.

V. TRANSMISSION CURVES

For many materials (weak absorbers) the semilogarithmic plot of the transmission curve was a simple straight line (see Fig. 4) indicating a constant cross section. Except for large $1/v$ absorbers a cross section so obtained was taken to be a potential or off resonance scattering cross section of the material at the detector energy.

Other materials (strong absorbers) (see Fig. 5)

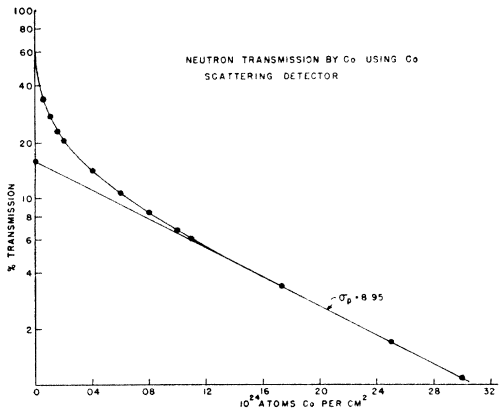

FIG. 2. Self-detected transmission curve of cobalt.

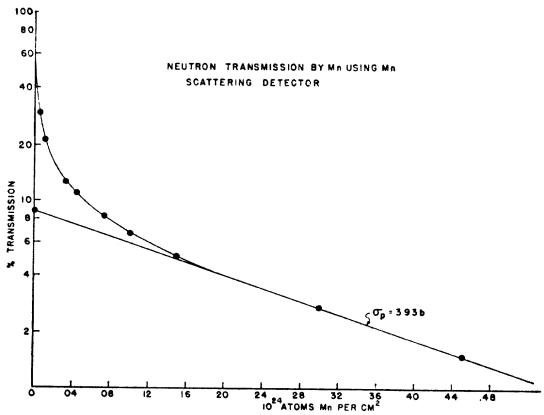

FIG. 3. Self-detected transmission curve of manganese.

TABLE I. Corrected values for σ_p, σ_i, σ_r, σ_c, and Δp for the elements measured to date.

	Co (115 ev)					Mn (300 ev)				
Element	σ_p 10^{-24} cm²	Δp %	σ_i 10^{-24} cm²	σ_r 10^{-24} cm²	σ_c 10^{-24} cm²	σ_p 10^{-24} cm²	Δp %	σ_i 10^{-24} cm²	σ_r 10^{-24} cm²	Comments
$_4$Be	6 07	100				6.04	100			
$_5$B	12.1	~100			~4.5	9.7	~100			Large capture
$_6$C	4.89	100			4.60	4.72	100			
$_8$O	4.08	100				4.15	100			Measured Al_2O_3
$_9$F	3.57	100				3.67	100			Measured CF_2
$_{12}$Mg	3.47	100				3.71	100			
$_{13}$Al	1.45	100				1.47	100			
$_{15}$P	4.11	100				4.16	100			
$_{16}$S	1.13	100				1.14	100			
$_{17}$Cl	~6.1	100				3.32	100			Large capture, measured CCl_4
$_{20}$Ca	4.56	100				4.37	100			Measured CaF_2
$_{22}$Ti	5.10	100				5.39	100			Beam attenuated only 35%
$_{24}$Cr	3.28	96	4.0	22	3.72	4.56	100			115 ev<Res<300 ev Measured Cr_2O_3
$_{25}$Mn	6.78	100			3.47	3.98	8.7	~3000		Detector
$_{27}$Co	9.30	16	~3000		7.35	7.23	91	11	38	Detector
$_{28}$Ni	16.6	100				15.6	100			
$_{29}$Cu	6.68	100				6.88	100			
$_{30}$Zn	3.91	100			4.23	3.74	87	7.8	35	Res>300 ev
$_{33}$As	6.22	96	9.1	77	6.90	7.20	80	15	44	115 ev<Res<300 ev
$_{34}$Se	8.11	100			8.60	11.3	100			
$_{35}$Br	9.66	77	29	93	7.89	8.94	89	16	72	Res<115 ev
$_{47}$Ag	6.21	88	22	135	8.98	6.43	92	10	57	Res_1>115 ev Res_2>300 ev
$_{48}$Cd	5.67	95	8.8	69	6.10	5.17	93	11	92	
$_{49}$In	5.84	95	9.6	81	6.85	6.06	95	10	89	
$_{50}$Sn	5.07	96	6.7	48	5.02	4.87	96	6.5	45	Small resonances
$_{51}$Sb	6.37	88	15	79	5.35	5.46	95	7.2	40	Res<115 ev
$_{52}$Te	5.17	100			5.48	5.05	95	9.2	87	Res>300 ev
$_{53}$I	4.19	97	10	214	5.15	4.64	94	9.4	99	Res_1>115 ev Res_2>300 ev
$_{58}$Ce	5.77	100				4.80	100			Measured CeO_2
$_{73}$Ta	11.3	90	32	217	10.7	9.60	83	28	118	Res_1<115 ev Res_2>300 ev
$_{74}$W	8.62	95	16	151	10.2	10.1	84	30	136	115 ev<Res<300 ev
$_{75}$Re	17.9	~100			15.0	15.2	68	56	143	Res near 300 ev Corrected for 0.1% Co Mn impurity <0.02%
$_{79}$Au	10.6	100			11.1	10.8	84	21	74	Res>300 ev
$_{80}$Hg	13.6	90	27	151	12.4	13.2	89	22	89	Res_1<115 ev Res_2<300 ev
$_{81}$Tl	9.52	100				11.7	83	18	46	Res near 300 ev Carbon correction small
$_{82}$Pb	11.1	100				10.7	100			
$_{83}$Bi	9.28	100				10.6	100			

proved to have considerable initial variation, Δi, in the transmission curve, but a well defined asymptotic component, Δp. Except for boron and chlorine, the slope of the asymptotic component was taken (when corrected by carbon, see below) to yield the potential (i.e., off resonance) cross section, or minimum cross section in the neighborhood of a resonance.

For those materials in which $\Delta i \neq 0$ it was important to determine what part of Δi was due to a variation in the cross section near the detector energy, and what part was due to a variation over the rest of the $1/E$ spectrum. That is, it was necessary to approximate the ideal resolving powers of the detectors in order to get their proper "local" indications. This was accomplished by measuring the transmission curve with a flat, i.e., carbon detector.

Consider Δi to be the sum of a resonance and a potential component

$$\Delta i = \delta r + \delta p,$$

δp may be determined from Δc (Δi for a C-detected transmission curve) and the detector resolving power

$$\delta p = p \Delta c,$$

where r/p = resolving power, and $r+p=1$. Then

$$\delta r = \Delta i - p \Delta c.$$

The transmission curves were corrected in this way thereby obtaining corrected values for σ_i, the initial cross section, σ_r, the difference cross section, and Δp, the percent asymptotic part of the transmission curve. These are related in a corrected transmission curve as follows:

$$\sigma_i = \delta r \cdot \sigma_r + \Delta p \cdot \sigma_p.$$

The difference cross section was labeled "σ_r" to indi-

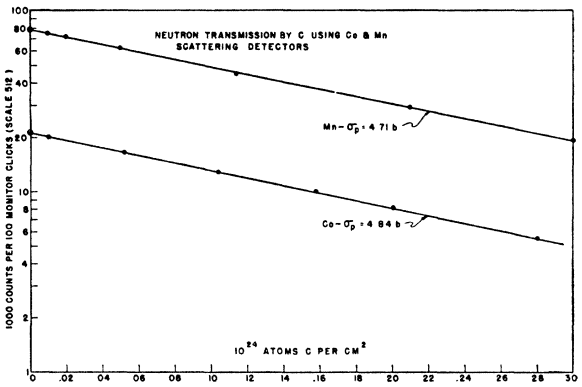

FIG. 4. Neutron transmission by carbon. Typical case where $\Delta i=0$.

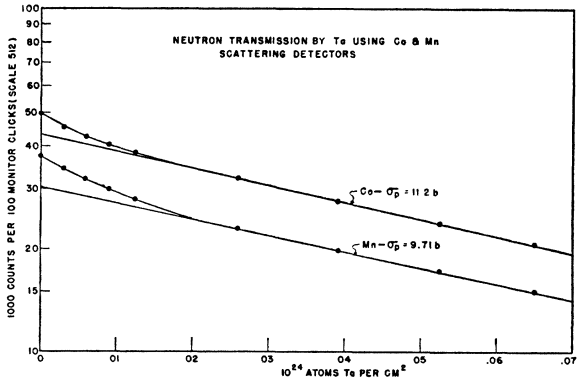

FIG. 5. Neutron transmission by tantalum. Typical case where $\Delta i\neq 0$.

cate it represented the effect of an overlapping resonance with the detector resonance.

To illustrate, consider the case of gold in which $\Delta c=35$ percent:

Co	Mn
$\Delta i=6$ percent	$\Delta i=20$ percent
$\delta p=0.18\times 35\simeq 6$ percent	$\delta p=.09\times 35\simeq 3$ percent
$\delta r=6-6\simeq 0$	$\delta r=20-3=17$ percent.

That is, for Au, there was no resonance overlapping with Co, but at the Mn resonance there was a resonance component of 17 percent in the transmission curve.

For $\Delta i\neq 0$, and for Se (large difference in σ_p between Co and Mn) the σ_p values were also corrected by a simple procedure. The uncorrected σ_p was considered to be a composite cross section determined as follows:

$$\sigma_p=p\sigma_c+r\sigma_p' \quad r+p=1$$

where σ_c is the asymptotic cross section of the C-detected transmission curve, and σ_p' is the corrected value of σ_p. The actual relations are given by:

$$\text{Co:}\quad \sigma_p'=\sigma_p+0.22(\sigma_p-\sigma_c)$$
$$\text{Mn:}\quad \sigma_p'=\sigma_p+0.10(\sigma_p-\sigma_c).$$

Since $\sigma_p\simeq\sigma_c$ these corrections were always <5 percent, and when $\Delta i=0$ were not made (except for Se) since they were ~ 1 percent. Table I lists corrected values for σ_p, σ_i, σ_r, σ_c and Δp for the elements measured to date.

VI. INTERPRETATION OF RESULTS

1. Asymptotic Cross Sections

The asymptotic cross sections were taken as proper off-resonance cross sections except in those cases in which non-resonance capture was present. In these cases (B and Cl) the asymptotic value for the Co detector was probably shifted to an energy higher than the Co resonance energy even though >90 percent of the neutrons scattered by Co (when corrected) lie within an energy band ± 10 ev of the Co resonance. The $1/v$ function is less steep at the Mn resonance, so one would expect less of a shift to higher energies in the measurement of σ_p with a Mn detector.

It should be noted that in a number of cases of resonance overlapping σ_p via Co or Mn detection was considerably less than σ_c. This lowest value of the cross section in the neighborhood of a resonance was interpreted as the cross section resulting from the interference of the resonance and potential scattering components. It indicated, too, that the detector resonance was of lower energy than the overlapping resonance in the absorber. In these cases σ_c should be a more proper value of the off-resonance or potential scattering cross section.

2. Initial Cross Sections

The initial cross sections (after correction) were taken to be proper average total cross sections (resonance capture+resonance scattering+potential scattering) of the absorber over the width of the detector resonance. $\delta r\neq 0$ (i.e., $\sigma_i>\sigma_p$) was taken as an indication of resonance overlapping with the detector.

3. Resonance Overlap Effect

Certain features of Table I should be observed:

(a) Resonance overlapping does not exist for the light elements. When it does set in overlapping occurs mainly for one detector (see As, Br).

(b) The heavy elements <Re exhibit overlapping essentially for both detectors.

(c) The heavy elements >Re exhibit less overlap effect. For example: Au overlaps only Mn, and Pb and Bi exhibit no overlapping. In this region of the table there may be interference from several resonance levels, resulting in small oscillations of the cross section.

(d) More data may make possible a statistical analysis of level density *vs.* Z and of σ_p *vs.* Z. The present data indicates that the ratio of the number of elements having the greatest overlap effect for Mn to those having the greatest overlap effect for Co is 2.5. This is approximately the ratio of detector energy widths.

(e) It should be noted that no resonance overlapping with Mn was found for Al,[4] and not enough for Cr[4] to credit the peaks shown by Rainwater, *et al.*, as real. They were probably due to Mn impurities.

[4] Columbia data, Rev. Mod. Phys. **19**, 271–274 (1947).